The Effect of Temperature, Precursor Concentration and Capping Group on the shape of CdS nanoparticles

N. Moloto,[a,b] N. Revaprasadu,[c] P. L. Musetha,[d] and M. J. Moloto[a*]

[a]*School of Chemistry, University of the Witwatersrand, Private Bag 3, Wits, 2050, RSA.*

[b]*National Centre for Nanostructured Materials, Council for Scientific and Industrial Research, PO Box 395, Pretoria, 0001, RSA.*

[c]*Department of Chemistry, University of Zululand, Private Bag X1001, KwaDlangezwa, 3886, RSA.*

[d]*University of Limpopo, Medunsa Campus, Medunsa, 0204, RSA.*

Abstract

A novel ligand to the synthesis of nanoparticles has been employed in this study. A Tetramethylthiuram disulphide cadmium complex (abundant in sulphur atoms) was used as a single-source precursor for the synthesis of CdS nanoparticles. The CdS nanoparticles were synthesized under various conditions and were characterized using UV/Vis, PL, XRD and TEM. The influence of the precursor concentration, temperature and capping environment as factors affecting the morphology and size of the nanoparticles was investigated. We observed that with an increase in precursor concentration, there was an increase in particle sizes and the morphology evolved from spherical to rod-shaped nanoparticles. An increase in temperature showed only evidence

of increasing the particle sizes whilst the capping environment had a profound influence on the morphology of the nanoparticles.

Keywords: Tetramethylthiuram disulphide, CdS nanocrystals, shape, morphology synthesis, precursor, precursor concentration, temperature, capping group.

Introduction

Tetramethylthiuram monosulfide and tetramethylthiuram disulfide, are compounds that are extensively used in the biomedical field[1]. The following thiuram derivatives; tetramethylthiuram disulphide (TMTD), tetraethylthiuram disulphide (TETD), tetramethylthiuram monosulphide (TMTM) and dipentamethylenethiuram disulphide (PTD) are sulphur containing compounds which speed up vulcanization, i.e. they are 'accelerators'[2]. Thiram (tetramethylthiuram disulphide) is used as a fungicide to protect seeds, fruit, vegetables, ornamentals, turf crops, and herbs from a variety of fungal diseases. In a biological study it was observed that thiram reacts with copper and lead metals to enhance the uptake of these metals by the roots of the plants while titanium and vanadium tend to reduce the thiram as a ligand to dithiocarbamates[3,4]. Complexes of thiodicarbonic diamide silver and mercury derivatives ($C_{12}H_{24}Ag_2Cl_2N_4S_6$, $C_6H_{12}AgN_3O_3S_3$, $C_{42}H_{42}AgN_2P_2S_3NO_3$ and $C_6H_{12}HgI_2N_2S_3$) are reported to have been prepared from the tetramethylthiuram monosulphide ligand, while the ligand tetramethylthiuram disulphide formed thioperoxydicarbonic diamide complexes of zirconium and dysprosium[5]. The use of these ligands as complexes with IIB metals, to

form precursors for II-VI semiconductor nanoparticles has attracted some interest, due to the presence of sulphur atoms. The thiuram disulphide unit consists of four sulfides and hence the binding to the metal centre upon formation of complexes would be through the sulfides. The stability of the complexes is enhanced by the chelating ability of the ligand to the metal ions. This resulted in an interest in tetramethylthiuram disulphide complexes of cadmium as potential single source precursors for the synthesis of CdS nanoparticles.

The fabrication of shape controlled nanoparticles and their self- assembly into materials still poses a challenge to many chemists and materials scientists. It is well documented that the shape of nanoparticles plays an important role in determining its properties[6-10]. One of the difficulties in preparation of 0D (spheres, cubes), 1D (rods, wires) and 2D (discs, prisms, plates) nanoparticles is the control of growth through variation of the reaction parameters[6-9]. Factors such as concentration, temperature, capping agent as well as the reaction time are critical parameters that influence the size and the morphology of the nanoparticles. Cheon and co-workers elucidated that these have an influence in the final outcome of the shapes of the nanoparticles[10]. Cheon *et al.*[10] argued that using high concentrations of precursor prolongs the time taken for the growth of the particles thus resulting in varying morphologies. They also showed that at different temperatures, different crystalline phases of CdS were favored resulting in growth at different crystal planes thus influencing morphology. By using surfactants that bind differently to the crystallographic faces, one can also control the shape of the nanocrystal[11]. At high temperatures (200 - 400 °C) the surfactant molecules are dynamically adsorbed to the surface of the growing crystal. The surfactant molecules must be mobile enough to provide access for the addition of the monomer units, stable enough to prevent

aggregation of the nanocrystals as well as at temperatures suitable for the synthesis. The choice of surfactants varies from case to case; a molecule that binds too strongly to the surface of the crystal is not suitable, as it would not allow the crystal to grow. On the other hand, a weakly coordinating molecule would yield large particles, or aggregates. At low temperatures, the surfactants are strongly bound to the surface of the nanocrystals and provide appreciable solubility in organic solvents[11-13]. For example, hexadecylamine (HDA) adsorbs selectively (with its amine) on the surface of the CdS favoring the formation of anisotropic morphology and appreciable solubility, compared with tri-*n*-octylphosphine oxide (TOPO)[13].

In this work we have successfully synthesized the tetramethylthiuram disulfide cadmium complex for use as a source of CdS nanoparticles. The precursor was thermolysed in HDA and TOPO using the established synthetic procedure as reported for various semiconductor nanoparticles[14-16]. The overall aim of this study is to validate the influence of factors such as concentration, reaction temperature and capping group on both size and morphology of CdS nanoparticles.

Experimental section

General

HDA (hexadecylamine), TOPO (tri-*n*-octylphosphine oxide) and TOP (tri octylphosphine) were purchased from Aldrich. Toluene and methanol were obtained from BDH. Toluene was stored over molecular sieves (40 Å, BDH) before use. Cadmium

chloride, tetramethylthiuram disulfide and ethanol (analytical grade) obtained from Aldrich, were used as purchased to prepare the precursors.

Optical characterization

A Perkin Elmer Lambda 20 UV-VIS Spectrophotometer was used to carryout the optical measurements and the samples were placed in silica cuvettes (1 cm, path length), using toluene as a reference solvent. A Jobinyvon-spex-Fluorolog-3-Spectrofluorimeter with a xenon lamp (150 W) and a 152 P photo multiplier tube as a detector was used to measure the photoluminescence of the particles. The samples were placed in quartz cuvettes (1-cm path length).

Electron microscopy

The Transmission Electron Microscopy (TEM) and High Resolution TEM images were obtained using a Philips CM 200 compustage electron microscope operated at 200 kV with a EDS analyzer. The samples were prepared by placing a drop of a dilute solution of sample in toluene on a silicon grid (400 mesh, agar). The samples were allowed to dry completely at room temperature.

X-Ray diffraction

X-Ray diffraction (XRD) patterns on powdered samples were measured on Phillips X'Pert materials research diffractometer using secondary graphite monochromated Cu Kα radiation (λ = 1.54060 Å) at 40 kV/ 50 mA. Samples were supported on glass slides.

Measurements were taken using a glancing angle of incidence detector at an angle of °2, for 2θ values over 20° – 60° in steps of 0.05° with a scan speed of 0.01 °2θ.s^{-1}.

Microanalysis

Microanalysis was performed on a CARLO ERBA elemental analyzer for C, H, N, S.

NMR and FT-IR spectroscopy

Infrared spectra were recorded on FT-IR Perkin Elmer paragon 1000 spectrophotometer using nujol mull. NMR spectra were recorded on a Varian Associates Inova spectrometer (400 and 300 MHz).

Thermogravimetry

Thermogravimetric analysis (TGA) was performed initially from 50 °C up to 800 °C on a Perkin Elmer Pyris 6 TGA with nitrogen flow and heating rate of 10 - 20 °C. min^{-1}.

(a) Synthesis of [$CdCl_2(SC(N(CH_3)_2)SS(N(CH_3)_2)CS))_2$]

A hot solution of tetramethylthiuram disulfide (1.00 g, 4.16 mmol) in methanol (20 mL) was added into a heated solution of cadmium chloride (0.38 g, 2.08 mmol) in methanol (15 ml). The mixture was stirred and refluxed for 1 h. The white precipitate was filtered, washed twice with methanol and dried under vacuum. Yield 74.8 %; m. p. 363.5 °C. $C_{12}H_{24}N_4Cl_2S_8Cd$: Anal. Calcd. C, 21.70; H, 3.64; N, 8.45. Found: C, 20.21; H 3.55; N 9.28. IR (nujol mull)/cm^{-1}: 1496(s), 1373(sh), 1234(s), 1126(s), 941(m). ^{1}H NMR (δ,

$CdCl_3$) ppm 4.10 (s, 3H), 3.92 (s, 3H); ^{13}C {^1H} NMR (δ, $CdCl_3$) ppm: 179.38 (s,CS); 31.22 (s, CH_3).

(b) Typical method of preparation of CdS nanoparticles

In a typical experiment, $[CdCl_2(SC(N(CH_3)_2)SS(N(CH_3)_2CS))_2]$ 1.0 g was dissolved in TOP (10 – 20 ml). This solution was then injected into 3.125 g of hot HDA at 180 or 240 °C, a decrease in temperature of 20 – 30 °C was observed. The solution was allowed to stabilize at 180 °C and heated for 60 minutes at this temperature. The solution was then allowed to cool to about 70 °C, and methanol was added to remove excess HDA. A flocculent precipitate formed and this solid product was separated by centrifugation and redispersed in toluene. Toluene was removed by evaporation under reduced pressure to give yellow HDA capped CdS nanoparticles. The particles were washed three times with methanol and redispersed in toluene. The following amounts were used with 1 g of precursor, 3.125 g, (1:1), 6.25 g (1:2), 12.5 g (1:4) and 25 g (1:8) of HDA and 6.25 g of TOPO.

Results and Discussion

Tetramethylthiuram disulfide

Thiram was used as a ligand in the synthesis of the complex in a 1: 2 mole ratio to yield a white product with melting point of 363.5 °C. The formation of the complex, $[CdCl_2(SC(N(CH_3)_2)SS(N(CH_3)_2CS))_2]$ was confirmed by elemental analysis, IR and NMR spectroscopy. The ligand coordinates to the metal through the sulfur atoms, thus making it possible for the use as a precursor in the synthesis of CdS nanoparticles.

Thermal decomposition of the cadmium complex of tetramethylthiuram disulfide in an inert atmosphere, led to the formation of metal sulfide in a main degradation step between 300 ºC and 370 ºC with a weight loss of about 68 % which correlates with the theoretical percentage of cadmium sulfide in the complex, 66.7%.

Effect of concentration

The ability to control and manipulate the physical and chemical properties of semiconductor nanoparticles depends upon the tuning of their size and shape. For example CdSe semiconductor crystals have characteristic red luminescence however on the sub 10 nm scale their luminescence can be tuned continuously from red to blue[12].

Figure 1 shows the absorption spectra of CdS nanoparticles prepared using varying amounts of concentration, i.e. from 1:1 to 1:8 (precursor: HDA) from the thiram precursor. The absorption spectra of particles with precursor to HDA, 1:8 (Figure 1a) and 1:4 (Figure 1b) show a blue-shift from the bulk band-edge of 515 nm, while the 1:2 and 1:1 (Figures 1c and d) show red-shifts in their band edges in relation to the bulk.. The band edges for the samples shown in Figure 1a – d are 502 nm, 510 nm, 515 nm and 525 nm respectively. The red-shift in band-edge is not characteristic of nanoparticles but could be explained using the reasoning reported by Cheon and co-workers[10]. Cheon discovered that not only the size of the nanoparticle has an influence on the band-gap but shape also plays an important role. In the case of rods, length and the width both have a contribution in the resultant band-edge. Therefore the red-shifts in band-edge can be

explained by the notion that the morphology of the particles has a great influence on the optical properties of the nanoparticles. With spherical particles, the diameter of the particle can be related to the whole size of the particle, whereas with rod- or wire-like particles, the diameter does not account for the length of the particles. This is consistent with the work done by Moloto *et. al*.[17], who reported similar trends with increasing precursor concentration. The photoluminescence spectra of the samples are shown in Figure 2. The emission maxima vary with the samples of different concentration and are red-shifted from their respective absorption band-edges. The emission peaks for all samples have an identical narrow shape, an indication of monodispersed particles that are well passivated. The presence of smooth single peaks is also indicative of the existence of predominantly single morphology.

The x-ray diffraction patterns of CdS nanoparticles prepared at the lowest precursor concentration and highest precursor concentration are shown in Figure 3. The XRD patterns of the CdS from the low precursor concentration exhibit the hexagonal phase; typical of spherical particles, whereas the CdS from the high precursor concentration shows a mixture of orthorhombic and cubic (Tables 1 and 2). The change in phases of the particles from lower concentration to higher concentration conforms to the change in their morphologies.

The TEM images in Figure 4 concur with the crystal phases obtained in the XRD and the absorption spectral features. As the concentration is increased the particles evolve from close to spherical to elongated shapes. The particles obtained from the lowest precursor

concentration (Figure 4a) are oblate in morphology. As precursor concentration is increased there is an appearance of rod-shaped particles (Figure 4b). A further increase shows the appearance of rods with a uniform aspect ratio (Figure 4c). At the highest concentration the rod-shaped particles are very distinct with a higher aspect ratio (Figure 4d). The concentration of the precursor influences the reaction pathway; the reaction can proceed either under a thermodynamic or kinetic growth control regime. The thermodynamic growth regime is driven by sufficient supply of thermal energy and low flux of monomers (low monomer concentration), yielding isotropic shaped, the most stable form of nanocrystals (e.g. cubes, spheres). In contrast under non-equilibrium, kinetic conditions with a relatively high flux of monomers, selective anisotropic growth (e.g. rod-like structures) between different crystallographic surfaces is facilitated[18-20].

Effect of temperature

Temperature is one of the major factors that influence the growth of the particles. The temperature of the reaction has an effect on the particle size with higher temperatures favoring larger sizes. The reaction temperature also affects the shape of the nanoparticles due to the competition between the kinetic and thermodynamic growth regime.

The precursor with a ratio of 1:4 was thermolysed at temperatures of 180 °C and 240 °C. The particles synthesized at 180 °C shows a blue shift in relation to the bulk material (Figure 5a). As the temperature is increased from 180 °C to 240 °C, there is a shift in the band-edge to the lower energies with tailing of the spectrum also observed (Figure 5b).

The TEM images of both samples are shown in Figure 6. The nanoparticles show similar morphologies of rod-shaped particles with a few spherical particles observed in the 180 °C sample. The observance of the rod-shaped particles confirms that the reaction is under kinetic control. The length and aspect ratio of the rods increases from 2.1 (180 °C) to 4.4 (240 °C) as a result of Ostwald ripening.

Effect of capping agent

In addition to HDA other organic capping groups such as tri-n-octylphosphine oxide (TOPO) and 4-ethylpyridine have been used in stabilizing the metal chalcogenide nanoparticles[21,22]. TOPO has been the original choice of capping group, pioneered by Bawendi *et. al.*[23]. It has been shown that variation of capping groups causes changes in particle morphology. Nair *et. al* [24] reported the synthesis of spherical TOPO capped CdS nanoparticles using a cadmium ethylxanthate as a precursor. Li *et. al*.[25] used the same precursor in HDA to observe rod shaped particles. The mode of interaction of the capping group is a crucial factor that tends to drive growth of particles along a particular plane making them more orientated towards a particular shape. It has also been shown by Alivisatos *et. al.*[26] that by changing the surface energies through adjustment of the types and ratios of organic surfactants the shape of CdSe nanoparticles could be controlled.

Figure 7, shows the absorption and emission spectra of TOPO capped CdS prepared under similar conditions (1:4 precursor to TOPO) as those of HDA-capped CdS nanoparticles in Figure 1(b) and 2(b). The absorption band edge was observed at 495 nm compared to the HDA capped particles (502 nm). The emission spectrum was broader

than the HDA capped particles. The XRD pattern showed peaks typical of the hexagonal phase (Figure 8). The TEM image showed close to spherical particles with an average size of 5 nm (Figure 9). The shape of the particles was in contrast to the rod shaped HDA capped particles synthesized under similar reaction conditions, confirming that the capping group plays a role in the morphology of the particles. The HDA molecule strongly binds on 100 plane of the nanoparticle, promoting growth along that axis whilst the TOPO molecule has not preferential facet.

Conclusions

CdS nanoparticles have been prepared by single source precursor method using tetramethylthiuram disulfide. The influence of concentration, temperature and capping agent to the final morphology of the nanoparticles was established. Larger precursor concentration resulted in 1D nanorods, whilst HDA-capped compared to the TOPO-capped nanoparticles resulted in the formation of rods. The temperature had the least profound influence on the morphology of the particles whilst a noticeable increase in particle size was observed.

References

1. J. G. Contreras, J. A. Gnecco, *Anales de Quimica*, 86, 740 (1990).

2. D. Adamczyk, *Environmental Engineering Science*, 23, 610 (2006).

3. L. I. Victoriano, Bol. Soc. Chil. Quím, 45, (2000).

4. I. Cuadrado, M. Morán, Trans. Met. Chem. 11, 375 (1986).

5. L. I. Victoriano, H. B. Cortes , M. I. S. Yuseff, L. C. Fuentealba , J. Coord. Chem. 39, 241 (1996) .

6. S. Yu, Jian Yang, Y. Qian, M. Yoshimura, Chem. Phys. Lett. 361, 362 (2002).

7. J. Yang, J. Zeng, S. Yu, L. Yang, G. Zhou, Y. Qian, Chem. Mater. 12, 3259 (2000).

8. J. Zhan, X. Yang, D. Wang, Adv. Mater. 12, 1348 (2000).

9. Y. Chen, J. Ding, Y. Guo, L. Kong, H. Li, Mater. Chem. Phys. 77, 734 (2002).

10. Y. Jun, J. Choi, J. Cheon, Angew. Chem. Int. Ed. 45, 3414 (2006).

11. E. C. Scher, L. Manna, A. P. Alivisatos, Phil. Trans. R. Soc. Lond. A 361, 241 (2003).

12. Y. Li, X. Li, C. Yang, Y. Li, J. Chem. Mater. 13, 2461 (2003).

13. L. Manna, E. Scher, A. P. Alivisatos, J. Cluster Science, 13, 521 (2002).

14. T. Trindade and P. O'Brien, Adv. Mater. 8, 161 (1996).

15. T. Trindade and P. O'Brien, Chem. Mater. 9, 523 (1997).

16. L. E. Brus, J. Chem. Phys. 79, 5566 (1983).

17. N. Moloto, N. Revaprasadu, M. J. Moloto, P. O'Brien, M. Helliwell, Polyhedron, 26, 3947 (2007).

18. X. Peng, Adv. Mater. 15, 459 (2003).

19. Z. A. Peng, X. G. Peng, J. Am. Chem. Soc. 124, 3343 (2002).

20. Y. Jun, Y. Jung, J. Cheon, J. Am. Chem. Soc. 124, 615 (2002).

21. M. J. Moloto, N. Revaprasadu, P. O'Brien, M. A. Malik, J. of Mater. Sci.: Mat. in Electr. 15, 313 (2004).

22. M. J. Moloto, N. Revaprasadu, G. A. Kolawole, P. O'Brien, M. A. Malik, S. Afr. J. Sci. 101, 463 (2005).

23. M. G. Bawendi, M. L. Steigerwald, L. E. Brus, Annu. Rev. Phys. Chem. 41, 477 (1990).

24. P. S. Nair, M. M. Chili, T. Radhakrishnan, N. Revaprasadu, P. Christian, P. O'Brien, S. Afr. J. Sci.101, 466 (2005).

25. Y. Li, X. Li, C. Yang, Y. Li, J. Chem. Mater. 13, 246 (2003).

26. X. G. Peng, L. Manna, W. D. Yang, J. Wickham, E. Scher, A. Kandavich, A. P. Alivisatos, Nature, 404, 59 (2000).

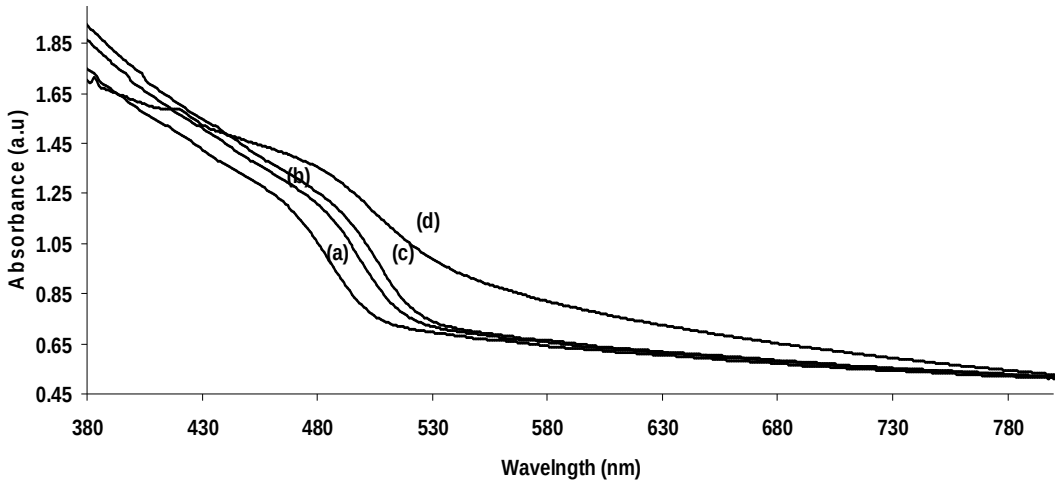

Figure 1: Absorption spectra of CdS nanoparticles at different precursor: HDA ratios (a) 1:8, (b) 1:4, (c) 1:2 and (d) 1:1.

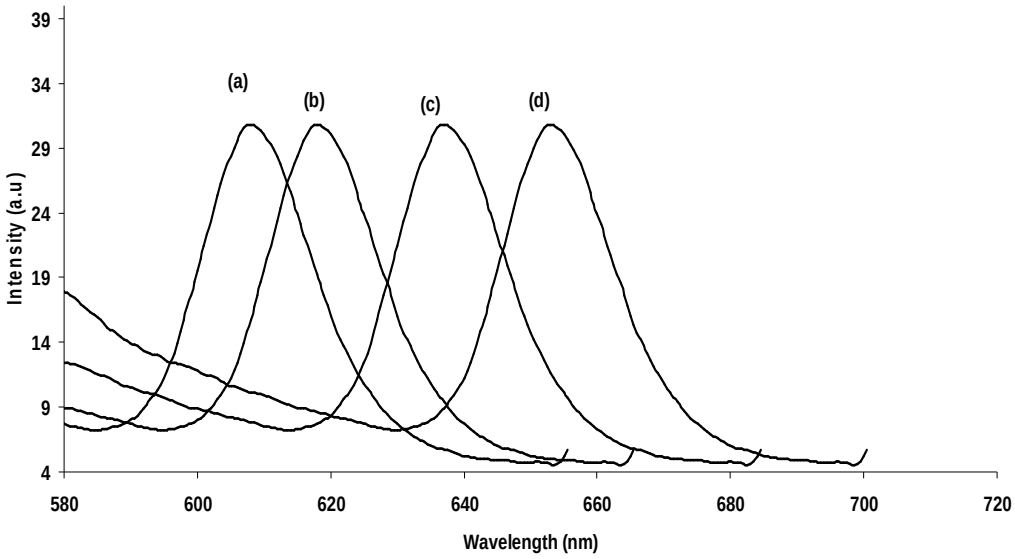

Figure 2: Emission spectra (PL) of CdS nanoparticles at different precursor: HDA ratios (a) 1:8, (b) 1:4, (c) 1:2 and (d) 1:1 (excitation 380 nm).

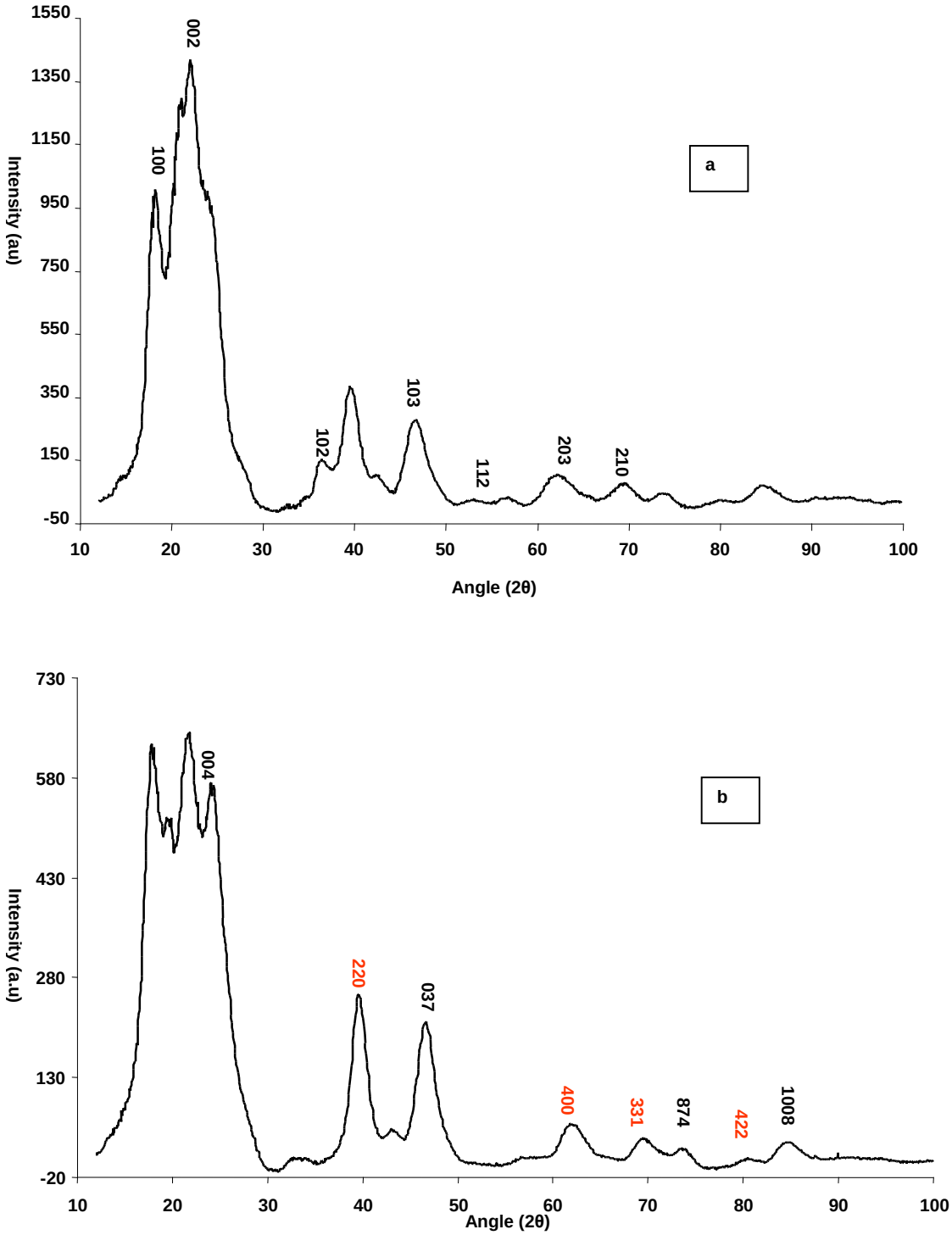

Figure 3: XRD of HDA capped CdS at (a) 1:8 and (b) 1:1 prepared at 180 °C.

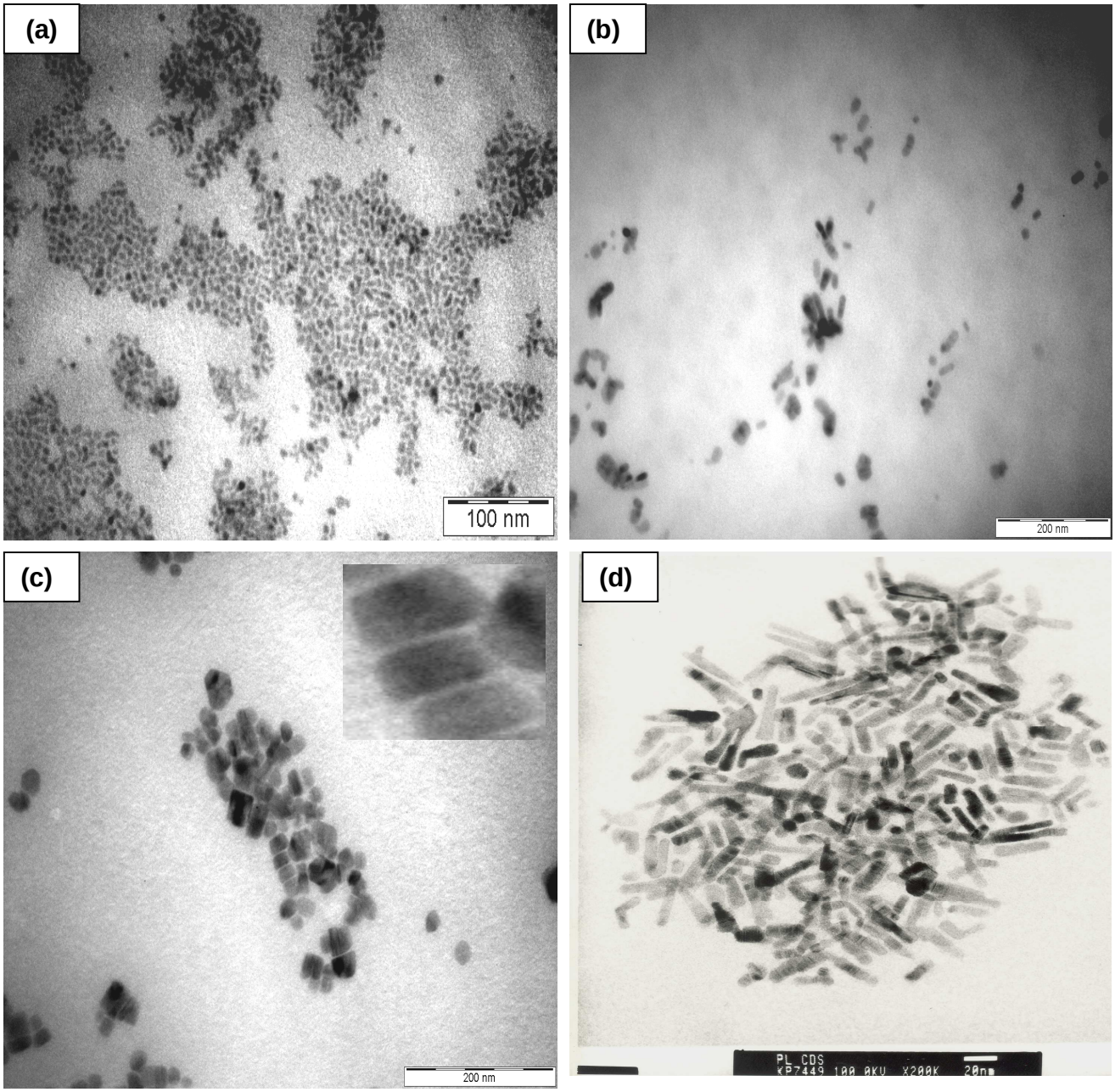

Figure 4: TEM image of CdS prepared at 180 °C, (a) 1:8, (b) 1:4, (c) 1:2 and (d) 1:1 precursor: HDA ratio.

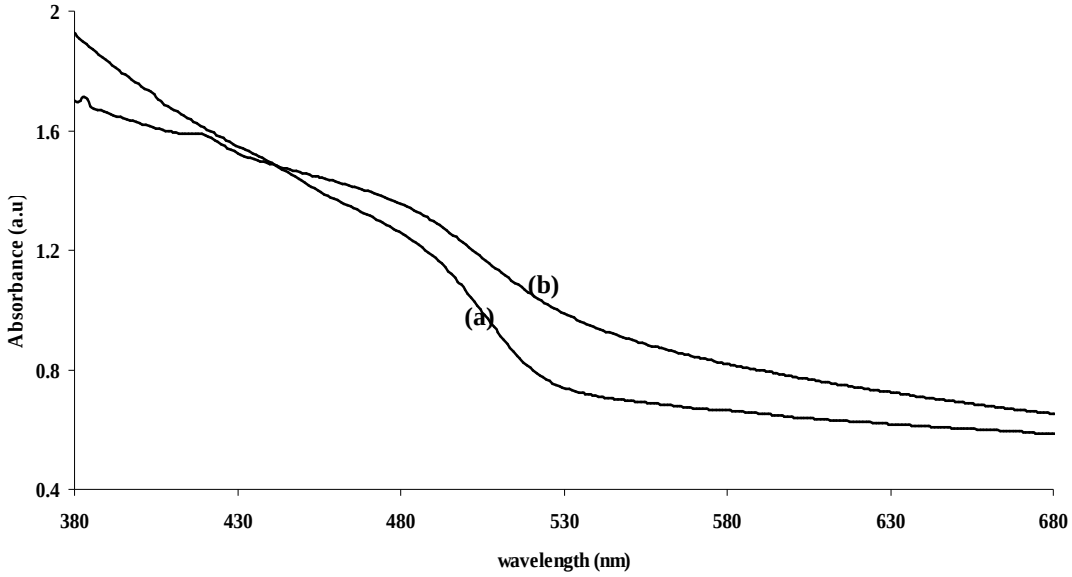

Figure 5: Absorption spectra of HDA capped CdS nanoparticles prepared at different temperatures (a) 180 °C and (b) 240 °C.

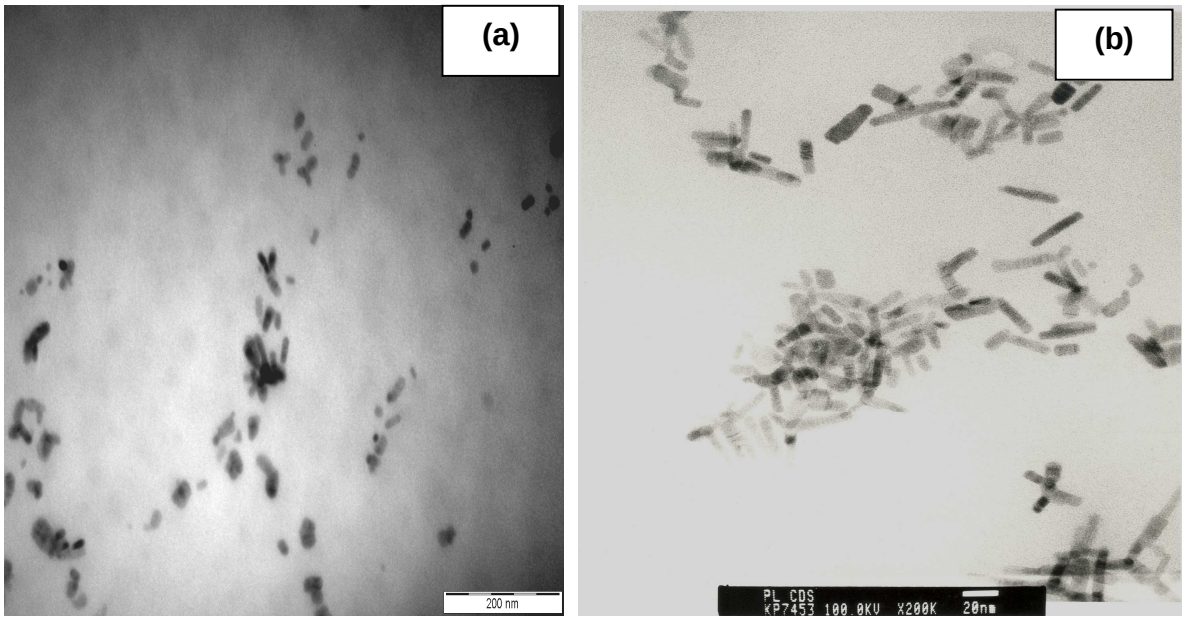

Figure 6: TEM image of CdS prepared at (a) 180 °C and (b) 240 °C, 1:4 ratio of precursor: HDA.

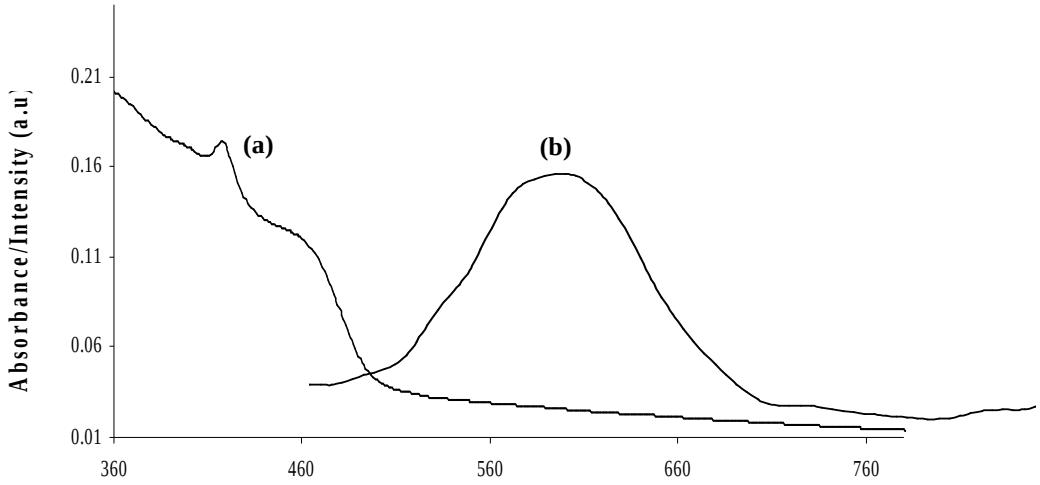

Figure 7: Absorption and PL spectra of TOPO capped CdS nanoparticles prepared at (1:2) 180 °C, (excitation 380 nm).

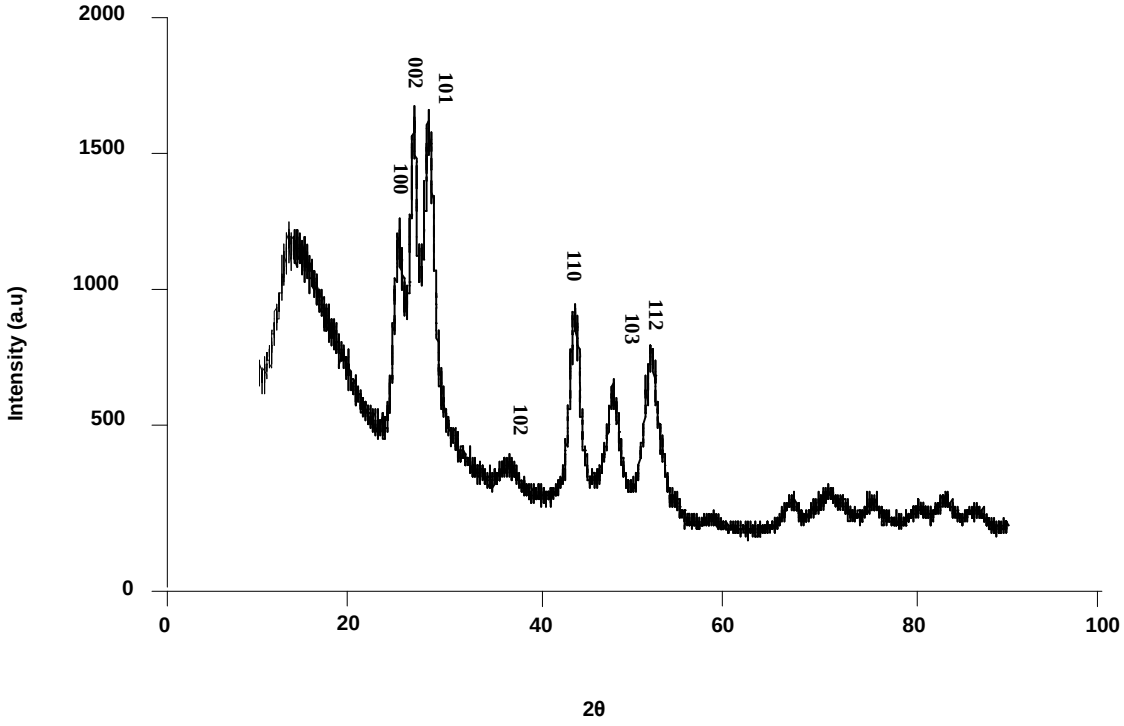

Figure 8: XRD of TOPO capped CdS (1:2) from thiram complex at 180 °C.

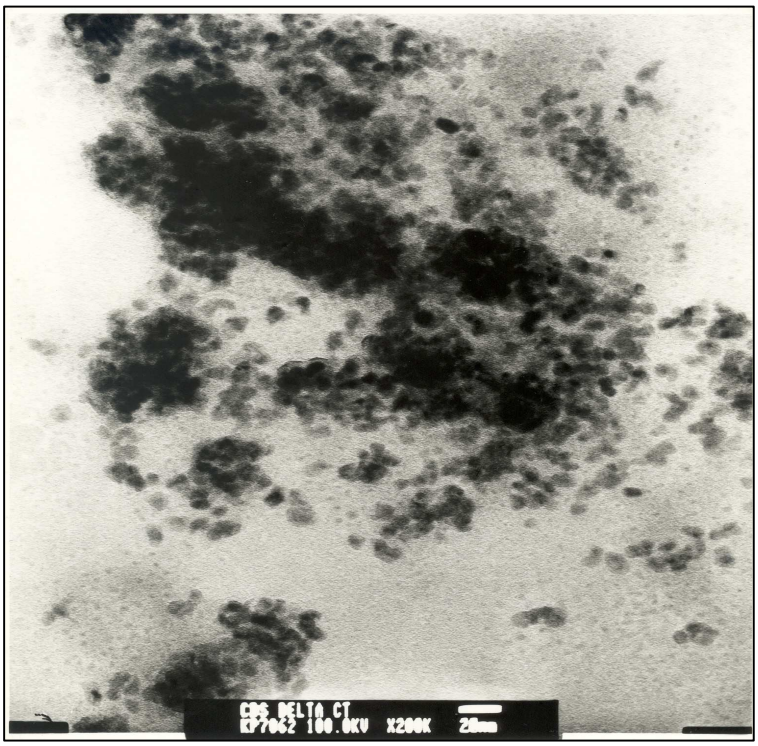

Figure 9: TEM image of TOPO-capped CdS (1:4).